Journal of Steroid Biochemistry & Molecular Biology 125 (2011) 57–65

Contents lists available at ScienceDirect

Journal of Steroid Biochemistry and Molecular Biology

journal homepage: www.elsevier.com/locate/jsbmb

Review

Selective inhibition of human 3β-hydroxysteroid dehydrogenase type 1 as a potential treatment for breast cancer

James L. Thomas[a,b,*], Kevin M. Bucholtz[d], Balint Kacsoh[a,c]

[a] Division of Basic Medical Sciences, Mercer University School of Medicine, 1550 College St, Macon, GA 31207, USA
[b] Department of Ob-Gyn, Mercer University School of Medicine, 1550 College St, Macon, GA 31207, USA
[c] Department of Pediatrics, Mercer University School of Medicine, 1550 College St, Macon, GA 31207, USA
[d] Department of Chemistry, Mercer University, Macon, GA, USA

ARTICLE INFO

Article history:
Received 18 May 2010
Received in revised form 2 July 2010
Accepted 12 August 2010

Keywords:
3β-Hydroxysteroid dehydrogenase
Short-chain dehydrogenase/reductase
Breast cancer
MCF-7 tumor cell
Enzyme inhibitor

ABSTRACT

Human 3β-hydroxysteroid dehydrogenase/isomerase type 1 (3β-HSD1) is a critical enzyme in the conversion of DHEA to estradiol in breast tumors and may be a target enzyme for inhibition in the treatment of breast cancer in postmenopausal women. Human 3β-HSD2 participates in the production of cortisol and aldosterone in the human adrenal gland in this population. In our recombinant human breast tumor MCF-7 Tet-off cells that express either 3β-HSD1 or 3β-HSD2, trilostane and epostane inhibit the DHEA-induced proliferation of MCF-7 3β-HSD1 cells with 12–16-fold lower IC_{50} values compared to the MCF-7 3β-HSD2 cells. Trilostane and epostane also competitively inhibit purified human 3β-HSD1 with 12–16-fold lower K_i values compared to the noncompetitive K_i values measured for human 3β-HSD2. Using our structural model of 3β-HSD1, trilostane was docked in the active site of 3β-HSD1, and Arg195 in 3β-HSD1 or Pro195 in 3β-HSD2 was identified as a potentially critical residue. The R195P-1 mutant of 3β-HSD1 and the P195R-2 mutant of 3β-HSD2 were created, expressed and purified. Kinetic analyses of enzyme inhibition suggest that the high-affinity, competitive inhibition of 3β-HSD1 by trilostane may be related to the presence of Arg195 in 3β-HSD1 versus Pro195 in 3β-HSD2. In addition, His156 in 3β-HSD1 may play a role in the higher affinity of 3β-HSD1 for substrates and inhibitors compared to 3β-HSD2 containing Try156. Structural modeling of the 3β-HSD1 dimer identified a possible interaction between His156 on one subunit and Gln105 on the other. Kinetic analyses of the H156Y-1, Q105M-1 and Q105M-2 support subunit interactions that contribute to the higher affinity of 3β-HSD1 for the inhibitor, epostane, compared to 3β-HSD2.

Article from the Special issue on Targeted Inhibitors.

Contents

* Corresponding author at: Division of Basic Medical Sciences, Mercer University School of Medicine, 1550 College St, Macon, GA 31207, USA.
Tel.: +1 478 301 4177; fax: +1 478 301 5489.
E-mail address: Thomas_J@mercer.edu (J.L. Thomas).

0960-0760/$ – see front matter © 2010 Elsevier Ltd. All rights reserved.
doi:10.1016/j.jsbmb.2010.08.003

1. Introduction

Human 3β-hydroxysteroid dehydrogenase/Delta 5→4-isomerase type 1 (3β-HSD1; short-chain dehydrogenase/reductase (SDR) nomenclature: 3BHS1_HUMAN or SDR11E1) and 3β-hydroxysteroid dehydrogenase/Delta 5→4-isomerase type 2 (3β-HSD2; SDR nomenclature: 3BHS2_HUMAN or SDR11E2) are encoded by two distinct genes which are expressed in a tissue-specific pattern [1,2]. Both isoforms of the enzyme catalyze the conversion of 3β-hydroxy-5-ene-steroids (dehydroepiandrosterone, 17α-hydroxypregnenolone, pregnenolone) to 3-keto-4-ene-steroids (androstenedione, 17α-hydroxyprogestrone, progesterone) on a single, dimeric protein containing both enzyme activities [3]. During human pregnancy, the placental enzyme catalyzes the conversion of pregnenolone to progesterone, which maintains the uterus in a quiescent state. Near term, however, the fetal zone adrenal gland produces large amounts (200 mg/day) of dehydroepiandrosterone (DHEA). Because the fetal adrenal lacks significant 3β-HSD/isomerase activity, the placental type 1 enzyme converts the fetal dehydroepiandrosterone to androstenedione. Androstenedione is converted by placental aromatase and 17β-hydroxysteroid dehydrogenase to estradiol, which participates in the cascade of events that initiates labor in humans [4]. In human breast cancer, circulating dehydroepiandrosterone-sulfate (DHEA-S) from the adrenal gland is converted by steroid sulfatase, 3β-HSD1, aromatase and 17β-HSD in the tumors and the surrounding normal mammary gland tissue to produce estradiol-17β (Fig. 1). In addition, estrone-sulfate is converted to estradiol-17β by steroid sulfatase and 17β-HSDs [5–8]. Inhibitors specific for 3β-HSD1 in mammary gland and breast tumors may inhibit tumor cell growth without affecting the activity of 3β-HSD2 in the adrenal gland [9–11]. To test that hypothesis, we have developed two recombinant (genetically engineered) human breast tumor MCF-7 cell lines that express either human 3β-HSD1 or 3β-HSD2 plus the other enzymes required for the biosynthesis of estradiol from DHEA-S. The 3β-HSD inhibitors, trilostane and epostane, competitively inhibit purified human 3β-HSD1 with 12–16-fold higher affinities compared to the noncompetitive inhibition of human 3β-HSD2 by these compounds [11–13]. The efficacies of inhibitors of 3β-HSD1 and aromatase have been compared as blockers of MCF-7 cell proliferation. The introduction of aromatase inhibitors (anastrozole, letrozole) has improved the prognosis of many breast cancer patients [14,15].

Another aim of our study has been to determine the functional significance of key non-identical amino acids of the two isoenzymes—Arg195 and His156 in 3β-HSD1 versus Pro195 and Tyr156 in 3β-HSD2 (two of 23 non-identical residues in the two isoenzymes). Docking studies of trilostane with our structural model of human 3β-HSD1 suggests that the 17β-hydroxyl group of the 3β-HSD inhibitor, trilostane (2α-cyano-4α,5α-epoxy-17β-ol-androstane-3-one), may interact with the Arg195 residue of 3β-HSD1 but not with Pro195 in 3β-HSD2. The R195P-1 mutant of 3β-HSD1 and the P195R-2 mutant of 3β-HSD2 were cre-

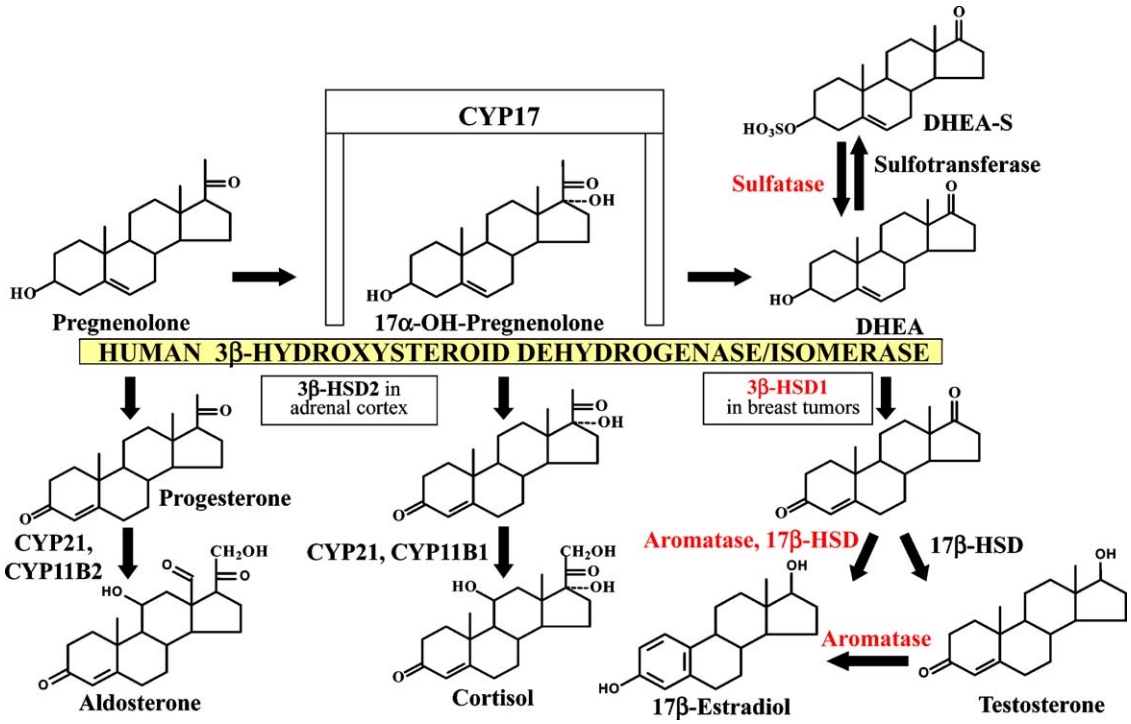

Fig. 1. Human 3β-hydroxysteroid dehydrogenase is expressed as two tissue-specific isoforms (3β-HSD1 and 3β-HSD2) as a key enzyme in the steroid biosynthetic pathways that produce estradiol, testosterone, cortisol and aldosterone. The enzymes that participate in the conversion of DHEA-S to 17β-estradiol in breast tumors are in red. (For interpretation of the references to color in this figure legend, the reader is referred to the web version of the article.)

Table 1
Levels of 3β-HSD1, 3β-HSD2 and aromatase mRNA in our genetically engineered human breast tumor MCF-7 Tet-off cells.

MCF-7 cells	3β-HSD1[a]	3β-HSD2	Aromatase
MCF-7 Tet-off (untransfected)	27	2	2
MCF-7 Tet-off 3β-HSD1	150,219	11	1
MCF-7 Tet-off 3β-HSD1 aromatase	108,804	3	43,186
MCF-7 Tet-off 3β-HSD1 aromatase dox	5780	3	43,405
MCF-7 Tet-off 3β-HSD2	35	138,511	2
MCF-7 Tet-off 3β-HSD2 aromatase	9	220,804	40,098
MCF-7 Tet-off 3β-HSD2 aromatase dox	30	2693	40,693

[a] Primers and probes specific for human 3β-HSD1, 3β-HSD2 and aromatase were used in these qRT-PCR studies. All data was normalized to 18s attomoles/μg RNA. All qRT-PCR measurements were performed in triplicate using the Applied Biosystems 7300 Real-time PCR system.

ated, expressed, purified and characterized kinetically to test this hypothesis [16]. In addition, we have reported [12] that His156 in 3β-HSD1 contributes to the 11–16-fold higher affinities that 3β-HSD1 exhibits for substrate (DHEA) and inhibitor (epostane) steroids compared to 3β-HSD2 with Tyr156 in the otherwise identical catalytic domains (Tyr154-Pro-His156/Tyr156-Ser-Lys158). Because our structural model localizes His156/Tyr156 in the subunit interface of 3β-HSD, the structural basis for the differences in 3β-HSD1 and 3β-HSD2 have been investigated using site-directed mutagenesis to determine if subunit interactions between Gln105 and His156 or Tyr156 are involved [11].

2. Methods and materials

2.1. Chemicals

Dehydroepiandrosterone (DHEA) was purchased from Sigma Chemical Co. (St. Louis, MO); reagent grade salts, chemicals and analytical grade solvents from Fisher Scientific Co. (Pittsburg, PA). The cDNA encoding human 3β-HSD1, 3β-HSD2 and aromatase was obtained from J. Ian Mason, Ph.D., Univeristy of Edinburgh, Scotland. Trilostane was obtained as gift from Gavin P. Vinson, DSc PhD, School of Biological Sciences, Queen Mary University of London. Epostane was obtained from Sterling-Winthrop Research Institute (Rensselaer, NY). Letrozole was obtained from Novartis Pharma AG (Basel, Switzerland). Glass distilled, deionized water was used for all aqueous solutions.

2.2. Real-time PCR (qRT-PCR) of the recombinant MCF-7 cells

Total RNA was isolated from the untransfected and recombinant MCF-7 Tet-off cell lines using the RNeasy Mini Kit, followed by Deoxyribonuclease I treatment (Qiagen, Valencia, CA). Single-strand cDNA was prepared from 2 μg of total RNA using High-Capacity cDNA Reverse Transcription Kit (Applied Biosystems, Foster City, CA). 3β-HSD1 and 3β-HSD2 primers and probes were used because of 93% sequence homology. Primers and probes specific for human 3β-HSD1, 3β-HSD2 and aromatase used in these qRT-PCR studies were described previously [13]. 3β-HSD1, 3β-HSD2 and 18s rRNA quantification were performed using Applied Biosystems TaqMan Gene Expression Master Mix. For aromatase quantification, SYBR Green I was used with Applied Biosystems Power SYBR Green PCR Master Mix. The cDNA product from 40 ng total RNA was used as template according to our published procedure [13]. Each gene mRNA expression level was calculated using the formula: ((attograms of gene mRNA measured by qRT-PCR relative to the cDNA standard curve)/(gene mRNA molecular weight))/(μg of control 18s rRNA) = attomoles of gene mRNA per μg 18s rRNA in Table 1.

2.3. Proliferation assays using the MCF-7 cells

The Clontech MCF-7 Tet-off cells transfected with the Tet-Off expression vector allows controlled expression of the human 3β-HSD1 or 3β-HSD2. The Clontech response plasmid, pTRE2hyg, containing cDNA encoding 3β-HSD1 or 3β-HSD2 was transfected into the MCF-7 Tet-off cells, and transfected clones were selected by incubation with hygromycin. In this stably transfected expression system, human 3β-HSD1 or 3β-HSD2 is produced in the MCF-7 cells, and the levels of 3β-HSD1 or 3β-HSD2 expression are maximal in the absence of doxycycline. In addition, the cDNA encoding human aromatase was cloned into the pCMVzeo mammalian expression vector, and the MCF-7 3β-HSD1 or 3β-HSD2 cells were stably tranfected with the aromatase gene, and transfected clones were selected by incubation with zeocin. These recombinant MCF-7 cells are plated in 96-well dishes (2000 cells/well) using RPMI medium without phenol red containing 10% charcoal dextran stripped FBS (Gemini Bio-Products, West Sacramento, CA).

To measure inhibition of 3β-HSD on the growth of our recombinant MCF-7 Tet-off 3β-HSD1 and 3β-HSD2 aromatase cells, the substrate, DHEA (5.0 nM, EC_{50}), and the 3β-HSD inhibitor, trilostane (0–2.5 μM) are added to the cultures in the presence (dox) and absence (no dox) of doxycycline (10 ng/ml). To measure inhibition of aromatase, the substrate steroid, DHEA (5.0 nM), and the aromatase inhibitor (letrozole, 0–20.0 nM) are added to the cultures in the presence (dox) and absence (no dox) of doxycycline (10 ng/ml). For each of these procedures, the hormones are introduced 48 h after the plates are seeded with the cells. After 4 days, the treatments and media are refreshed. On day 10 after cell plating, the MTT dye is added to measure a viable cell count by colorimetric assay (absorbance at 595 nm). Our standard curves determined that an increase or decrease in 0.1 absorbance units at 595 nm measures an increase or decrease of 8000 MCF-7 cells in each well of the 96-well plate that hold 20,000 MCF-7 cells at confluency. Each value reported is the mean of 4 independent determinations ± SD.

2.4. Bioinformatics/computational biochemistry/graphics

As described previously [17], a three-dimensional model of human 3β-HSD1 has been developed based upon the X-ray structures of two related SDR enzymes: the ternary complex of *Escherichia coli* UDP-galactose 4-epimerase (UDPGE) with NAD^+ cofactor and substrate (PDB AC: 1NAH) [18] and the ternary complex of human 17β-hydroxysteroid dehydrogenase type 1 (17β-HSD1) with NADP and androstenedione (PDB AC: 1QYX) [19]. In this spliced model, the 153 residue N-terminal sequence comprising the NAD^+ binding site of 3β-HSD1 better matches that of UDPGE (52% homology). The substrate portion of the 3β-HSD1 active site (residues 154–255) better matches that of 17β-HSD1 (55% homology), which shares steroid ligand specificity and hydroxysteroid dehydrogenase function with 3β-HSD1 [17]. Amino acid sequence alignments were performed using CLUSTAL W (1.81) multiple sequence alignment [20].

This PDB file for 3β-HSD1 was used in Autodock 3.0 (The Scripps Research Institute, http://autodock.scripps.edu) [21] after the 17β-HSD product steroid was removed, leaving the NAD^+ cofactor in the binding site. All docking experiments were carried out using Autodock 3.0 using the Genetic Algorithm with Local Searching. Independent runs (256) were carried out and the docking results were then analyzed by a ranked cluster analysis. Compounds were identified that had the lowest overall binding energy. The three-dimensional graphics of 3β-HSD1 or the R195P-1 mutant docked with trilostane were created using the DeepView Swiss-PdbViewer (http://www.exspasy.org/spdbv/) for the protein with ligands and using Adobe Photoshop Elements (San Jose, CA) for text labeling.

2.5. Site-directed mutagenesis

Using the Advantage cDNA PCR kit (BD Biosciences Clontech, Palo Alto, CA) and pGEM-3βHSD1 or pGEM-3βHSD2 as template, double-stranded PCR-based mutagenesis produced the mutant cDNA for the 3β-HSD mutants, R195P-1, P195R-2, H156Y-1, Q105M-1 and Q105M-2, as described previously [11,12,16]. The presence of the mutated codon and integrity of the entire mutant 3β-HSD cDNA were verified by automated dideoxynucleotide DNA sequencing using the Big Dye Terminator Cycle Sequencing Ready Reaction kit (Applied Biosystems, Foster City, CA).

2.6. Expression and purification of the mutant and wild-type enzymes

The mutant R195P-1, P195R-2, H156Y-1, Q105M-1, Q105M-2, wild-type 3β-HSD1 or 3β-HSD2 cDNA was introduced into baculovirus and expressed in Sf9 cells as previously described [22]. Recombinant baculovirus was added to 1.5×10^9 Sf9 cells (1 L) at a multiplicity of infection of 10 for expression of each mutant enzyme. The expressed mutant and wild-type enzymes were separated by SDS-polyacrylamide (12%) gel electrophoresis, probed with anti-3β-HSD polyclonal antibody (Novus Biologicals, Littleton, CO) and detected using the ECL western blotting system with anti-goat, peroxidase-linked secondary antibody (Amersham Pharmacia Biotech, Piscataway, NJ). Each expressed enzyme was purified from the 100,000 × *g* pellet of the Sf9 cells (4 L) by our published method [3] using Igepal CO 720 (Rhodia, Inc., Cranbury, NJ) instead of the discontinued Emulgen 913 detergent (Kao Corp, Tokyo). Each expressed, purified mutant and wild-type enzyme produced a single major protein band (42.0 kDa) on SDS-polyacrylamide (12%) gel electrophoresis that co-migrated with the purified human 3β-HSD1 control enzyme. Protein concentrations were determined by the Bradford method using bovine serum albumin as the standard [23].

2.7. Kinetic studies

Michaelis–Menten kinetic constants for the 3β-HSD substrate were determined for the purified mutant and wild-type enzymes in incubations containing dehydroepiandrosterone (DHEA, 2–100 μM) plus NAD^+ (0.2 mM) and purified enzyme (0.03 mg) at 27 °C in 0.02 M potassium phosphate, pH 7.4. The slope of the initial linear increase in absorbance at 340 nm per min (due to NADH production) was used to determine 3β-HSD1 activity. Kinetic constants for the isomerase substrate were determined at 27 °C in incubations of 5-androstene-3,17-dione (20–100 μM), with NADH (0.05 mM) and purified enzyme (0.02 mg) in 0.02 M potassium phosphate buffer, pH 7.4. Isomerase activity was measured by the initial absorbance increase at 241 nm (due to androstenedione formation) as a function of time. Blank assays (zero-enzyme, zero-substrate) assured that specific isomerase activity was measured as opposed to non-enzymatic, "spontaneous" isomerization (Thomas et al. [3]). Changes in absorbance were measured with a Varian (Sugar Land, TX) Cary 300 recording spectrophotometer. The Michaelis–Menten constants (K_m, V_{max}) were calculated from Lineweaver–Burke (1/*S* versus 1/*V*) plots and verified by Hanes–Woolf (*S* versus *S*/*V*) plots. The k_{cat} values (min^{-1}) were calculated from the V_{max} values (nmol/min/mg) and represent the maximal turnover rate (nmol product formed/min/nmol enzyme dimer).

Inhibition constants (K_i) were determined for the inhibition of the 3β-HSD1, 3β-HSD2, H156Y-1, Q105M-1, Q105M-2, R195P-1 and R195P-2 activities by trilostane or epostane using conditions that were appropriate for each enzyme species based on substrate K_m values. For 3β-HSD1, the incubations at 27 °C contained sub-saturating concentrations of DHEA (4.0 μM or 8.0 μM), NAD^+ (0.2 mM), purified human type 1 enzyme (0.03 mg) and trilostane or epostane (0–1.0 μM) in 0.02 M potassium phosphate buffer, pH 7.4. For 3β-HSD2, similar incubations contained DHEA (8.0 μM or 20.0 μM) and trilostane or epostane (0–10.0 μM). For the mutant enzymes, similar incubations contained DHEA substrate and inhibitor noted in the legends of Tables 3 and 4. Dixon analysis (*I* versus 1/*V*) was used to determine the type or mode of inhibition (competitive, noncompetitive) and calculate the inhibition constant (K_i) values. The K_i value represents the inhibitor concentration that reduces maximal enzyme activity by 50% and is considered a measure of the affinity of the enzyme for the inhibitor. A decrease in K_i indicates an increase in affinity [24].

Our triplicate determinations of the kinetic constants used highly purified mutant and wild-type enzymes to produce very reliable results with little variation between the values. The standard deviations reported for the mean values in the kinetic tables show that the variation between triplicates is 5–9%. With such low variation in the kinetic determinations, the observed differences of 2–16-fold between the kinetic constants of mutant and wild-type enzymes for substrates, cofactors and inhibitor analogs are interpreted to represent real differences.

3. Results

3.1. qRT-PCR, western blot analysis and proliferation assays that assess enzyme levels in the recombinant MCF-7 cells

The key to measuring the specificity of inhibitors for 3β-HSD1 in proliferation assays using our recombinant MCF-7 cells is validation that our MCF-7 Tet-off 3β-HSD1 aromatase cells express no human 3β-HSD2 and the MCF-7 Tet-off 3β-HSD2 aromatase cells express negligible endogenous human 3β-HSD1. Our qRT-PCR results shown in Table 1 provide definitive evidence that our recombinant MCF-7 cells meet these criteria. In addition, doxycycline (Dox) turns off (56–82-fold decrease) the expression of 3β-HSD1 or 3β-HSD2 (as expected for stable transfection using the Clontech Tet-off response plasmid, pTRE2hyg). Comparing the levels of transfected 3β-HSD1 in our recombinant MCF-7 cells to those found in human breast tumors is not possible due to a lack of comparable data in the literature. However, it has been reported that induction of human 3β-HSD1 in human breast tumor ZR-75-1 (ER+) and BT-20 (ER−) cells activity by IL-4 and IL-13 increases the formation of estrogen precursors and may have a significant impact on the estrogen biosynthesis in breast tumors, plus no 3β-HSD2 was detected in these cells [9]. Table 1 also shows that the MCF-7 Tet-off 3β-HSD1 and 3β-HSD2 cell lines have been stably transfected with human aromatase, which is not affected by Dox as expected for stable transfection with pCMVzeo-aromatase. As shown by the qRT-PCR results in Table 1, the Clontech Tet-off MCF-7 cells express no endogenous aromatase mRNA and required transfection with pCMVzeo-aromatase to provide this enzyme activity.

As reported using our anti-steroid sulfatase and anti-17β-HSD1 antibodies, human steroid sulfatase and 17β-HSD1 were determined by western immunoblots to be present as endogenous enzymes in the MCF-7 cells [13]. In the same report, estrone (EC_{50} = 0.39 nM) or estradiol (EC_{50} = 0.24 nM) stimulated the growth of the MCF-7 Tet-off 3β-HSD1 aromatase and of the MCF-7 Tet-off 3β-HSD2 aromatase cells (estrone EC_{50} = 0.34 nM; estradiol EC_{50} = 0.32 nM) at very similar rates, which indicates that endogenous 17β-HSD reductase activity is present in the parent Clontech MCF-7 Tet-off cells [13]. Similar proliferation assays using DHEA-S, DHEA and androstenedione demonstrated concentration-dependent stimulation of the growth of our MCF-7 Tet-off 3β-HSD1 aromatase and MCF-7 Tet-off 3β-HSD2 aromatase, which further

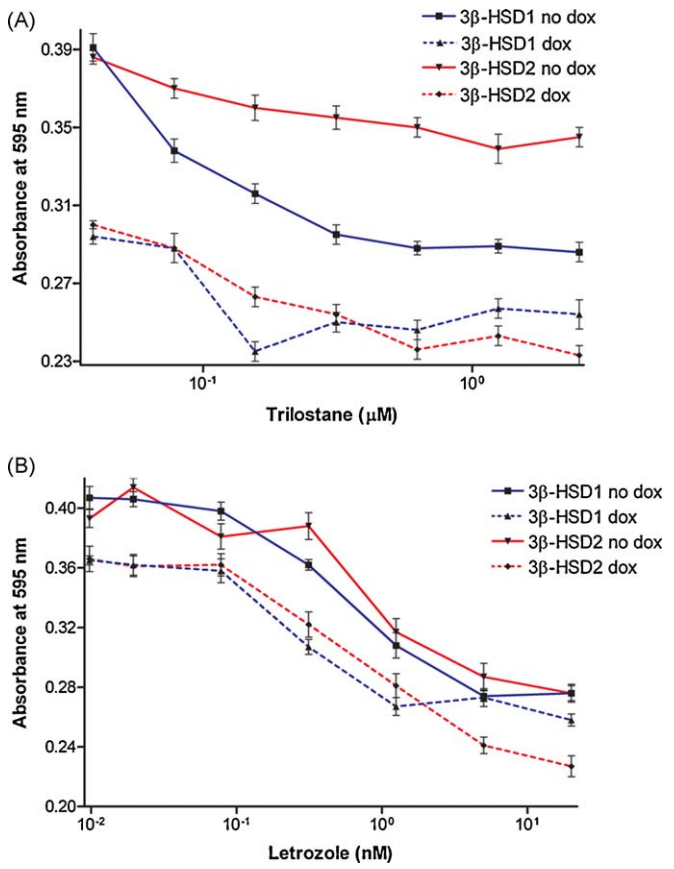

Fig. 2. Inhibition of the proliferation of genetically engineered MCF-7 breast tumor cells by trilostane or letrozole. (A) The 3β-HSD inhibitor, trilostane (0–2.5 μM) slows the DHEA-stimulated (5 nM) proliferation of our recombinant MCF-7 Tet-off 3β-HSD1 aromatase cells in the absence (no dox, ■, solid line) and presence of 10 ng/ml doxycycline (dox, ▲, broken line) and recombinant MCF-7 Tet-off 3β-HSD2 aromatase cells in the absence (no dox, ▼, solid line) and presence of doxycycline (dox, ♦, broken line). (B) The aromatase inhibitor, letrozole (0–20.0 nM), decreases the DHEA-stimulated (5 nM) proliferation of the recombinant MCF-7 Tet-off 3β-HSD1 aromatase cells in the absence (no dox, ■, solid line) or presence of 10 ng/ml doxycycline (dox, ▲, broken line) and of the recombinant MCF-7 Tet-off 3β-HSD2 aromatase cell lines in the absence (no dox, ▼, solid line) or presence of doxycycline (dox, ♦, broken line) as described in Section 2. Each value is the mean of 4 independent determinations ± SD. Assays are conducted as described in Section 2. Each value is the mean of 4 independent determinations ± SD.

supported the presence of steroid sulfatase, 3β-HSD, aromatase and 17β-HSD in our MCF-7 cell model [13]. Our MCF-7 cell proliferation results with DHEA-S or DHEA as substrate were similar to those reported for MCF-7 cells in the past [25].

3.2. Inhibition of 3β-HSD1 or aromatase slows the growth of the MCF-7 cells

As shown in Fig. 2A, the 3β-HSD inhibitor, trilostane, slows the proliferation of our MCF-7 Tet-off 3β-HSD1 aromatase cells (IC_{50} = 0.3 μM) with a 16-fold higher affinity compared to the MCF-7 Tet-off 3β-HSD2 aromatase cells (IC_{50} = 4.9 μM). When doxycycline (dox) is present to turn-off the expression of 3β-HSD1 or 3β-HSD2, the basal stimulation of proliferation by substrate (DHEA at 5.0 nM, mean EC_{50} [13]) is substantially reduced, and the inhibition of the growth of both MCF-7 cell lines by trilostane is greatly attenuated. The related 3β-HSD inhibitor, epostane, also selectively inhibits the growth of our MCF-7 Tet-off 3β-HSD1 aromatase cells (IC_{50} = 0.2 μM) with a 12-fold higher affinity relative to the MCF-7 Tet-off 3β-HSD2 aromatase cells (IC_{50} = 2.4 μM) [13]. These results mirror the inhibition of 3β-HSD1 by epostane or trilostane with 12–16-fold higher affinity than 3β-HSD2 that was measured with the purified isoenzymes as well as in homogenates of our recombinant MCF-7 3β-HSD1 and MCF-7 3β-HSD2 cells [10,11]. In Fig. 2B, the aromatase inhibitor, letrozole, inhibits the DHEA-stimulated proliferation of the MCF-7 Tet-off 3β-HSD1 aromatase (IC_{50} = 0.6 nM) and MCF-7 Tet-off 3β-HSD2 aromatase (IC_{50} = 0.9 nM) cell lines at similar rates with little change in rate observed in incubations containing doxycycline (dox), as expected for the inhibition of aromatase in these cells. Neither trilostane nor letrozole stimulated the proliferation of the MCF-7 cells in the absence of DHEA substrate, so none of these compounds has ER-agonist activity in our breast tumor cell model.

3.3. Targeting the key residues using the structural model and docking analysis

The targeting of Arg195/Pro195 in 3β-HSD1/3β-HSD2 is based on the docking results obtained with our structural model of human 3β-HSD1, which has 51% homology of the Rossmann-fold domain (residues 1–200) and 40% identity of the key fingerprint residues that interact with bound substrate and cofactor compared to the crystallographic structure of *E. coli* UDP-galactose-4-epimerase with the substrate domain of human 17β-hydroxysteroid dehy-

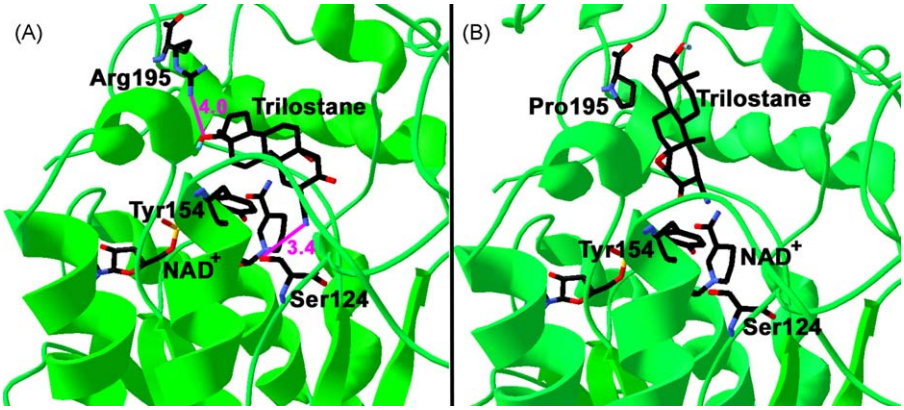

Fig. 3. Docking of trilostane with our structural model of human 3β-HSD1. (A) The proposed interaction between the 17β-hydroxyl group of trilostane and the guanidinium group of the Arg195 residue of the wild-type enzyme (4.0 Å) and the apparent proximity of the anchoring hydroxyl group of the Ser124 residue to the 2α-cyanogroup of docked trilostane (3.4 Å) are shown. (B) Docking of trilostane with the R195P mutant of 3β-HSD1 (containing Pro195) shows a binding shift of the inhibitor compared to the orientation of trilostane docked with wild-type 3β-HSD1 containing Arg195 in Panel A. The illustrations of catalytic residues, Tyr154 and Ser124, and cofactor, NAD^+, indicate that this view represents the active site of the enzyme. The protein backbone (green), carbon (black), oxygen (red) and nitrogen (blue) atoms plus estimated bond distances (magenta) are shown. (For interpretation of the references to color in this figure legend, the reader is referred to the web version of the article.)

Table 2
Comparison of Michaelis–Menten constants of substrates for purified human 3β-HSD1, R195P-1, 3β-HSD2 and P195R-2.

Purified enzyme	3β-HSD[a]			Isomerase[b]		
	K_m (μM)	k_{cat} (min^{-1})	k_{cat}/K_m (min^{-1} μM^{-1})	K_m (μM)	k_{cat} (min^{-1})	k_{cat}/K_m (min^{-1} μM^{-1})
R195P-1	10.7	7.7	0.72	63.2	64.2	1.02
3β-HSD1	3.7	3.3	0.89	27.9	50.2	1.80
P195R-2	7.7	5.6	0.73	101.8	87.5	0.86
3β-HSD2	15.6	8.7	0.44	88.4	81.4	0.92

[a] Kinetic constants for the 3β-HSD substrates were determined spectrophotometrically (340 nm) in incubations containing DHEA or 16β-hydroxy-DHEA (1–100 μM), NAD^+ (0.2 mM) and purified enzyme (0.04 mg) in 0.02 M potassium phosphate, pH 7.4.
[b] Kinetic constants for the isomerase substrate were determined in incubations of 5-androstene-3,17-dione (17–150 μM), NADH (0.05 mM) and purified enzyme (0.02 mg) in 0.02 M potassium phosphate buffer, pH 7.4.

drogenase type 1 (17β-HSD1) [17]. Site-directed mutagenesis has supported the function of the catalytic residues and selected substrate, cofactor and inhibitor binding residues as suggested by the structural model in previous studies [11,12,17,26–28]. However, we recognize the limitations of using our structural model of human 3β-HSD1 in the docking studies. The bond distances noted below between the docked trilostane and the protein amino acids or NAD^+ (in the crystal structures of the enzymes used in the model) should be considered to be estimates in the absence of an actual crystallographic structure of 3β-HSD1 with each bound steroid ligand. The structural model only suggests which amino acids to target, and the functions of these residues are then tested by mutagenesis and kinetic analyses.

Trilostane was docked in the active site of our structural model of human 3β-HSD1 and the chimeric R195P-1 mutant of 3β-HSD1 (containing Pro195 as in 3β-HSD2) using Autodock 3.0. As shown in Fig. 3A, the 17β-hydroxyl group of trilostane is proposed to interact with the R-guanidinium group of Arg195 (4.0 Å) in wild-type 3β-HSD1. Docking with the R195P-1 mutant suggests that Pro195 in 3β-HSD2 does not function as a recognition residue for the 17β-hydroxyl group of trilostane (Fig. 3B). To test our proposal that Arg195 functions as a key recognition residue for the high-affinity inhibition of 3β-HSD1 by trilostane, the R195P-1 mutant of 3β-HSD1 and the P195R-2 mutant of 3β-HSD2 have been created, expressed, purified and characterized.

The presence of His156 in human 3β-HSD1 versus Tyr156 in 3β-HSD2 has been shown to participate in the 11–16-fold greater affinity of the type 1 enzyme for 3β-HSD substrate steroids and inhibitors compared to the 3β-HSD2 [12]. We have localized the critical His156 residue in the subunit interface of the 3β-HSD1 enzyme dimer by homology modeling (Fig. 4) and tested this prediction by mutagenesis of the potential key hydrogen-binding partner, Gln105, on the other subunit of 3β-HSD1 and 3β-HSD2 to produce Q105M-1 and Q105M-2, respectively. Tyr156 is not shown in Fig. 4 (same position as His156). This cartoon is a representation of the proposed anti-parallel subunit interface (discussed below) and is not the result of docking analysis.

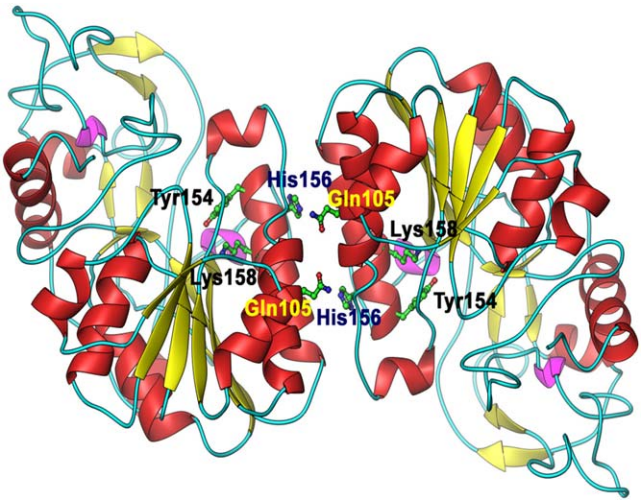

Fig. 4. Homology model of the human 3β-HSD1 dimer showing the hydrogen-binding residues, Gln105 and His156, in the subunit interface as well as the catalytic residues, Tyr154 and Lys158, in the active site. In the similar human 3β-HSD2 dimer interface, Tyr156 replaces His156 (not shown).

3.4. Substrate and inhibition kinetic analyses of the R195P-1 and P195R-2 mutant enzymes

Comparisons of the Michaelis–Menten values of DHEA as substrate of 3β-HSD1, 3β-HSD2, R195P-1 and P195R-2 are shown in Table 2. The R195P-1 mutation shifted the DHEA substrate kinetics to the lower affinity profile of 3β-HSD2, and the P195R-2 shifted substrate kinetics to the higher affinity profile of 3β-HSD1. The isomerase substrate kinetics were less affected by the mutations at position 195 than those observed for 3β-HSD (Table 2). The cofactor kinetics were not affected by either the R195P-1 or P195R-2 mutation [16].

Dixon analyses of the inhibition of the R195P-1 mutant, P195R-2 mutant, wild-type 3β-HSD1 and wild-type 3β-HSD2 by trilostane have measured inhibition constants (K_i values in Table 3) that support a role for Arg195 in the competitive inhibition of 3β-HSD1 by trilostane with a 16-fold lower K_i compared to the noncompetitive inhibition of 3β-HSD2 with Pro195 at this position in the protein. The R195P-1 mutation shifts the high-affinity, competitive inhibition profile of 3β-HSD1 to a low-affinity (K_i = 2.56 μM), noncompetitive inhibition profile similar to that of 3β-HSD2 containing Pro195. The P195R-2 mutation shifts the low-affinity, noncompetitive inhibition profile of 3β-HSD2 to a high-affinity (K_i = 0.19 μM), competitive inhibition profile similar to that of 3β-HSD1 containing Arg195 (Table 3).

Table 3
Comparison of inhibition constants of trilostane for purified human R195P-1, 3β-HSD1, P195R-2 and 3β-HSD2.

Enzyme	Trilostane K_i (μM)[a]
R195P-1	2.56 ± 0.22
3β-HSD1	0.10 ± 0.01 (C)
P195R-2	0.19 ± 0.02 (C)
3β-HSD2	1.60 ± 0.10

[a] For 3β-HSD1 and P195R-2, the incubations contained subsaturating concentrations of DHEA (4.0 μM or 8.0 μM), NAD^+ (0.2 mM), purified human 3β-HSD type 1 enzyme (0.04 mg) and trilostane (0–1.0 μM) in 0.02 M potassium phosphate buffer, pH 7.4. For 3β-HSD2 and R195P-1, similar incubations contained DHEA (8.0 μM or 20.0 μM) and trilostane (0–7.5 μM). Dixon analysis (I versus $1/V$) was used to determine the mode of inhibition and calculate the K_i values. (C) Denotes a competitive mode of inhibition, and no notation indicates a noncompetitive mode of inhibition. Values from the triplicate experiments are shown using mean ± SD.

Table 4
Inhibition and substrate kinetics for the 3β-HSD and isomerase activities of the purified mutant H156Y-1, Q105M-1, Q105M-2 and wild-type enzymes.

Purified enzyme	3β-HSD[a]				Isomerase[b]		
	K_i [c] (μM)	K_m (μM)	k_{cat} (min^{-1})	k_{cat}/K_m (min^{-1} μM^{-1})	K_m (μM)	k_{cat} (min^{-1})	k_{cat}/K_m (min^{-1} μM^{-1})
Q105M-1	1.84	40.5	6.8	0.17	33.0	34.8	1.06
H156Y-1	1.18	42.4	7.1	0.17	27.9	54.6	1.96
3β-HSDl	0.07	3.7	3.3	0.89	27.9	50.2	1.25
Q105M-2	1.64	25.0	4.5	0.18	80.8	66.7	0.82
3β-HSD2	0.98	47.3	7.1	0.15	88.4	81.5	0.92

[a] Kinetic constants for the 3β-HSD substrate (DHEA) were determined in incubations at 27 °C containing NAD^+ (200 μM), dehydroepiandrosterone (3–100 μM) and purified enzyme (0.04 mg) in 0.02 M potassium phosphate, pH 7.4. Each K_m and k_{cat} value represents the mean of triplicate measurements with a standard deviation ≤7% of single mutant enzyme preparations.

[b] Kinetic constants for the isomerase substrate (5-androstene-3,17-dione) were determined in incubations at 27 °C of NADH (50 μM), 5-androstene-3,17-dione (20–100 μM) and purified enzyme (0.01–0.04 mg) in 0.02 M potassium phosphate buffer, pH 7.4.

[c] Inhibition constants (all K_i values from Dixon plots) for inhibition of the purified enzymes by epostane were determined in spectrophotometric assays at 340 nm (3β-HSDl: epostane = 0–0.75 μM; 3β-HSD2, Q105M, H156Y: epostane = 0–7.5 μM).

3.5. Substrate and inhibition kinetic analyses of the mutant H156Y-1, Q105M-1, Q105M-2 enzymes

The Michaelis–Menten kinetic values measured for substrate utilization by purified H156Y-1, Q105M-1, Q105M-2, 3β-HSD1, and 3β-HSD2 are summarized in Table 4. For the dehydrogenase activity, the Q105M-1 mutant demonstrates an 11-fold higher K_m for substrate and 2-fold higher k_{cat} than 3β-HSD1, which are similar to those of 3β-HSD2 and to those measured for the H156Y-1 mutant enzyme. The Q105M-2 mutant exhibits DHEA kinetic constants that are similar to those of 3β-HSD2 with almost identical utilization efficiencies (k_{cat}/K_m). The Q105M-1 and Q105M-2 mutant enzymes retain isomerase substrate K_m values similar to the appropriate 3β-HSD1 or 3β-HSD2 isoform. Both Q105 M mutant enzymes exhibit reduced isomerase activity (k_{cat}) compared to their wild-type enzyme counterpart.

The inhibition constant values (K_i values in Table 4) derived from Dixon analyses (I versus $1/V$) show that epostane inhibits the 3β-HSD activity of H156Y-1 and Q105M-1 with 16–26-fold lesser affinities compared to the K_i values measured using the wild-type 3β-HSD1 enzyme. However, Q105M-2 retains the lower affinity profile of inhibition by epostane that are observed with wild-type 3β-HSD2 (Table 4).

4. Discussion

Human 3β-HSD/isomerase is a complex, multifunctional steroidogenic enzyme that is unique because it is membrane-bound in both smooth endoplasmic reticulum (microsomes) and mitochondria [3], utilizes NAD^+ but not $NADP^+$ as a coenzyme [28] and has a definitive tissue-specific expression of the 3β-HSD1 (mammary gland, breast tumors, placenta, skin) and 3β-HSD2 (adrenal gland, ovary, testis) isoforms [1]. Although the 3β-HSD activity is capable of performing the oxidation or reduction of substrate steroids, the irreversible 5 → 4-ene-steroid isomerase activity on the same protein allows the conversion of 3β-hydroxy-5-ene-steroid substrates to 3-keto-4-ene-product steroids but not the reduction of the 3-keto-4-ene-product steroid. A 3-keto-5-ane-steroid can be reduced, however, because the isomerization reaction is not involved [29].

Human 3β-HSD1 has been overlooked as a target enzyme for inhibition in the treatment of breast cancer [30]. That is most likely due to the presence of two isoforms in the human female. 3β-HSD1 is expressed in mammary gland and breast tumors, while 3β-HSD2 is expressed in the adrenal gland and ovary [31]. Because the inhibition of adrenal 3β-HSD2 would block the production of cortisol and aldosterone in postmenopausal women, these unwanted effects tend to overshadow the value of inhibiting 3β-HSD1 in breast tumors to block estradiol production. However, we have shown that the classic 3β-HSD inhibitors, trilostane and epostane, competitively inhibit purified human 3β-HSD1 with much higher affinity compared to human 3β-HSD2 [11–13]. To determine if this high-affinity inhibition of purified 3β-HSD1 translates into the selective inhibition of the growth of human breast tumors, we developed recombinant MCF-7 Tet-off breast tumor cells that express either 3β-HSD1 or 3β-HSD2 as well as the other enzymes required to produce estradiol from DHEA-S. Epostane or trilostane (Fig. 2A) inhibit the DHEA-induced proliferation of MCF-7 3β-HSD1 aromatase cells with 12–16-fold lower IC_{50} values compared to the MCF-7 3β-HSD2 aromatase cells, which correlate well with the relative K_i values obtained with purified 3β-HSD1 and 3β-HSD2 [13]. DHEA-S can also be converted by steroid sulfatase and 17β-HSD1 in breast tumors to 5-androstene-3β,17β-diol, which is a partial agonist of the estrogen receptor [31]. However, trilostane and epostane have been shown to be specific inhibitors of 3β-HSD and to have no effect on other enzymes in steroidogenesis (e.g., 17β-HSD) [32,33], so inhibition of the production of 5-androstene-3β,17β-diol does not appear to responsible for the inhibition of the MCF-7 cell growth in our studies. Trilostane has been shown to be metabolized by humans in vivo to an active metabolite, 17-keto-trilostane (2α-cyano-4α,5α-epoxy-androstane-3,17-one), which may account for a portion of the inhibition of MCF-7 cell proliferation [34]. These results with 3β-HSD1 inhibitors equal the effects of the aromatase inhibitor, letrozole, on MCF-7 cell proliferation (Fig. 2B), correlate well with the results obtained for inhibition of the purified isoenzymes and suggest that development of more highly selective 3β-HSD1 inhibitors may produce effective treatments for hormone-sensitive breast cancer.

A focus of our research has been to identify non-identical amino acid residues in 3β-HSD1 and 3β-HSD2 that may be responsible for the higher affinity of 3β-HSD1 for substrate and inhibitor steroids. Two key amino acid differences have been identified: His156 and Arg195 in 3β-HSD1 versus Tyr156 and Pro195 in 3β-HSD2. Introduction of the H156Y-1 mutation in 3β-HSD1 shifted the high-affinity substrate and inhibitor kinetic profile of 3β-HSD1 to the low-affinity kinetic profile of wild-type 3β-HSD2 containing Tyr156 [12]. However, His156 and Tyr156 are on the α-helix containing the catalytic Tyr154 and Lys158 in 3β-HSD and oriented on the opposite side of the enzyme-active site [11,12]. Our homology model predicts that Gln105 is positioned to hydrogen-bond to the imidazole ring of His156 across the subunit interface of 3β-HSD1, and to hydrogen-bond to the phenolic group of Tyr156 on the adjacent subunit of 3β-HSD2. In this model, the subunits are anti-parallel relative to each other at a helical interface, as has been reported for human 17β-HSD1 [19] and *E. coli* UDP-galactose-4-epimerase [18]. Based on a cataloging of interactions between Gln-His and Gln-Tyr residues in high resolution protein crystal

structures, the Gln-Tyr side chain interactions are tightly clustered in only a few geometries compared to the extensive range of geometries observed for side chain interactions between Gln and His [35]. Thus, the Q105M-1 mutation may disrupt key hydrogen-bonding interactions between Gln105 and His156 in the subunit interface of 3β-HSD1. However, the Q105M-2 mutation has little effect because the Gln105-Tyr156 hydrogen-bond may either not exist or is relatively weak between the subunits of 3β-HSD2 due to the restrictive geometry of this interaction [36]. The 11-fold higher K_m for the dehydrogenase substrate and the 16–26-fold lower K_i values of epostane measured for H156Y-1 and Q105M-1 compared 3β-HSD1 in this study are very similar [11]. In sharp contrast, the Q105M-2 mutant exhibits substrate and inhibitor kinetics of both the dehydrogenase and isomerase activities that are similar to those of 3β-HSD2, which emphasizes the different interactions between the subunits of the two isoforms. Subunit interactions may be critical to the binding orientation of the substrate steroid in the adjacent catalytic sites containing Tyr154 and Lys158. Thus, the interactions between Gln105 and His156 in the subunit interface of 3β-HSD1 appear to be key structural reasons for its 11–26-fold higher affinity for the DHEA dehydrogenase substrate and inhibitor steroids relative to 3β-HSD2. In addition, the Q105M-1 mutant data supports our model of the anti-parallel orientation of the two 3β-HSD1 monomers.

Using our well-validated structural model [17], docking analyses have identified two key residues in human 3β-HSD that may interact with trilostane in the active site of the enzyme. In our recent study [37], Ser124 in both 3β-HSD1 and 3β-HSD2 was suggested to interact with the 2α-cyanoketone group of trilostane by docking analyses, and this prediction was supported by site-directed mutagenesis and characterization of the purified S124T mutant enzyme. Docking followed by mutagenesis and kinetic characterization has suggested that Arg195 in 3β-HSD1 and Pro195 in 3β-HSD2 is a critical difference in the two isoenzymes. These studies support key interactions of Arg195 and Ser124 in 3β-HSD1 with the side-chains of docked trilostane (Fig. 3A). The inhibition kinetics of the R195P-1 mutant of 3β-HSD1 and the P195R-2 mutant of 3β-HSD2 strongly support an interaction between the Arg195 residue in human 3β-HSD1 and the 17β-hydroxyl group of trilostane that may be a major structural factor responsible for the high-affinity, competitive inhibition of human 3β-HSD1 compared to the low-affinity, noncompetitive inhibition of 3β-HSD2 (containing Pro195). Based on the selective inhibition of 3β-HSD1 and 3β-HSD mutants by trilostane or epostane as reported in this review, the development of new 3β-HSD1 inhibitors that exploit structural differences in the two human isoenzymes or of small interference RNA (siRNA) that selectively interfere with the expression of 3β-HSD1 [38] may lead to new treatments for hormone-dependent breast cancer.

Acknowledgments

This research was supported by NIH grant CA114717 (JLT). We thank Gavin P. Vinson, DSc PhD, School of Biological Sciences, Queen Mary University of London, for the providing the trilostane and for helpful comments.

References

[1] E. Rheaume, Y. Lachance, H.-F. Zhao, N. Breton, M. Dumont, Y. de Launoit, C. Trudel, V. Luu-The, J. Simard, F. Labrie, Structure and expression of a new complementary DNA encoding the almost exclusive 3 beta-hydroxysteroid dehydrogenase/delta 5-delta 4-isomerase in human adrenals and gonads, Mol. Endocrinol. 5 (8) (1991) 1147–1157.

[2] B. Persson, Y. Kallberg, J.E. Bray, E. Bruford, S.L. Dellaporta, A.D. Favia, R.G. Duarte, H. Jörnvall, K.L. Kavanagh, N. Kedishvili, M. Kisiela, E. Maser, R. Mindnich, S. Orchard, T.M. Penning, J.M. Thornton, J. Adamski, U. Oppermann, The SDR (short-chain dehydrogenase/reductase and related enzymes) nomenclature initiative, Chem. Biol. Interact. 178 (1–3) (2009) 94–98.

[3] J.L. Thomas, R.P. Myers, R.C. Strickler, Human placental 3β-hydroxy-5-ene-steroid dehydrogenase and steroid 5-4-ene-isomerase: purification from mitochondria and kinetic profiles, biophysical characterization of the purified mitochondrial and microsomal enzymes, J. Steroid Biochem. 33 (2) (1989) 209–217.

[4] B. Kacsoh, Endocrine Physiology, McGraw-Hill Companies, Inc., New York, 2000, pp. 566–567.

[5] T.M. Penning, M.E. Burczynski, J.M. Jez, C.F. Hung, H.K. Lin, H. Ma, M. Moore, N. Palackal, K. Ratnam, Human 3alpha-hydroxysteroid dehydrogenase isoforms (AKR1C1-AKR1C4) of the aldo–keto reductase superfamily: functional plasticity and tissue distribution reveals roles in the inactivation and formation of male and female sex hormones, Biochem. J. 351 (1) (2000) 67–77.

[6] J.R. Pasqualini, G.S. Chetrite, The selective estrogen enzyme modulators in breast cancer, in: J.R. Pasqualini (Ed.), Breast Cancer. Prognosis, Treatment and Prevention, Marcel Dekker, New York, 2002, pp. 187–249.

[7] M.J. Reed, A. Purohit, Breast cancer and the role of cytokines in the regulating estrogen synthesis: an emerging hypothesis, Endocr. Rev. 18 (5) (1997) 701–715.

[8] D. Ghosh, P. Vihko, Molecular mechanism of estrogen recognition and 17-keto reduction by 17β-hydroxysteroid dehydrogenase type 1, Chem. Biol. Interact. 130–132 (1–3) (2001) 637–650.

[9] S. Gingras, R. Moriggl, B. Groner, J. Simard, Induction of 3beta-hydroxysteroid dehydrogenase/delta5-delta4 isomerase type 1 gene transcription in human breast cancer cell lines and in normal mammary epithelial cells by interleukin-4 and interleukin-13, Mol. Endocrinol. 13 (1) (1999) 66–81.

[10] J.L. Thomas, T.C. Umland, L.A. Scaccia, E.L. Boswell, B. Kacsoh, The higher affinity of human type 1 3β-hydroxysteroid dehydrogenase (3β-HSD1) for substrate and inhibitor steroids relative to human 3β-HSD2 is validated in MCF-7 tumor cells and related to subunit interactions, Endocr. Res. 30 (4) (2004) 935–941.

[11] J.L. Thomas, E.L. Boswell, L.A. Scaccia, V. Pletnev, T.C. Umland, Identification of key amino acids responsible for the substantially higher affinities of human type 1 3β-hydroxysteroid dehydrogenase/isomerase (3β-HSD1) for substrates, coenzymes and inhibitors relative to human 3β-HSD2, J. Biol. Chem. 280 (22) (2005) 21321–21328.

[12] J.L. Thomas, J.I. Mason, S. Brandt, B.R. Spencer, W. Norris, Structure/function relationships responsible for the kinetic differences between human type 1 and type 2 3β-hydroxysteroid dehydrogenase and for the catalysis of the type 1 activity, J. Biol. Chem. 277 (45) (2002) 42795–42801.

[13] J.L. Thomas, K.M. Bucholtz, J. Sun, V.L. Mack, B. Kacsoh, Structural basis for the selective inhibition of human 3β-hydroxysteroid dehydrogenase 1 in human breast tumor MCF-7 cells, Mol. Cell. Endocrinol. 302 (1–2) (2009) 174–182.

[14] R.J. Santen, S.J. Santner, R.J. Pauley, L. Tait, J. Kaseta, L.M. Demers, C. Hamilton, W. Yue, J.P. Wang, Estrogen production via the aromatase enzyme in breast carcinoma—which cell type is responsible, J. Steroid Biochem. Mol. Biol. 61 (3–6) (1997) 267–271.

[15] E.P. Winer, C. Hudis, H.J. Burstein, A.C. Wolff, K.I. Pritchard, J.N. Ingle, R.T. Chlebowski, R. Gelber, S.B. Edge, J. Gralow, M.A. Cobleigh, E.P. Mamounas, L.J. Goldstein, T.J. Whelan, T.J. Powles, J. Bryant, C. Perkins, J. Perotti, S. Braun, A.S. Lange, G.P. Browman, M.R. Somerfield, ASCO technology assessment on the use of aromatase inhibitors as adjuvant therapy for postmenopausal women with hormone receptor-positive breast cancer: status report 2004, J. Clin. Oncol. 23 (3) (2005) 1–9.

[16] J.L. Thomas, V.L. Mack, J. Sun, J.R. Terrell, K.M. Bucholtz, The functions of key residues in the inhibitor, substrate and cofactor sites of human 3β-hydroxysteroid dehydrogenase type 1 are validated by mutagenesis, J. Steroid Biochem. Mol. Biol. 120 (4–5) (2010) 192–199.

[17] V.Z. Pletnev, J.L. Thomas, F.L. Rhaney, L.S. Holt, L.A. Scaccia, T.C. Umland, W.L. Duax, Rational proteomics V: structure-based mutagenesis has revealed key residues responsible for substrate recognition and catalysis by the dehydrogenase and isomerase activities in human 3β-hydroxysteroid dehydrogenase/isomerase type 1, J Steroid Biochem. Mol. Biol. 101 (1) (2006) 50–60.

[18] J.B. Thoden, P.A. Frey, H.M. Holden, Crystal structures of the oxidized and reduced forms of UDP-galactose 4-epimerase isolated from *Escherichia coli*, Biochemistry 35 (16) (1996) 2557–2566.

[19] R. Shi, S.X. Lin, Cofactor hydrogen bonding onto the protein main chain is conserved in the short chain dehydrogenase/reductase family and contributes to nicotinamide orientation, J. Biol. Chem. 279 (16) (2004) 16778–16785.

[20] J.D. Thompson, D.G. Higgins, T.J. Gibson, CLUSTAL W: improving the sensitivity of progressive multiple sequence alignment through sequence weighting, position specific gap penalties and weight matrix choice, Nucleic Acids Res. 22 (22) (1994) 4673–4680.

[21] G.M Morris, D.S. Goodsell, R.S. Halliday, R. Huey, W.E. Hart, R.K. Belew, A.J. Olson, Automated docking using a lamarckian genetic algorithm and empirical binding free energy function, J. Comput. Chem. 19 (14) (1998) 1639–1662.

[22] J.L. Thomas, B.W. Evans, G. Blanco, R.W. Mercer, J.I. Mason, S. Adler, W.E. Nash, K.E. Isenberg, R.C. Strickler, Site-directed mutagenesis identifies amino acid residues associated with the dehydrogenase and isomerase activities of human type I (placental) 3β-hydroxysteroid dehydrogenase/isomerase, J. Steroid Biochem. Mol. Biol. 66 (5–6) (1998) 327–334.

[23] M.M. Bradford, A rapid and sensitive method for the quantitation of microgram quantities of protein utilizing the principle of protein-dye binding, Anal. Biochem. 72 (May) (1976) 248–254.

[24] I.H. Segel, Enzyme Kinetics: Behavior and Analysis of Rapid Equilibrium and Steady-State Enzyme Systems, John Wiley & Sons, New York, 1993, pp. 109–111.
[25] Billich, P. Nussbaumer, P. Lehr, Stimulation of MCF-7 breast cancer cell proliferation by estrone sulfate and dehydroepiandrosterone sulfate: inhibition by novel non-steroidal steroid sulfatase inhibitors, J. Steroid Biochem. Mol. Biol. 73 (5) (2000) 225–235.
[26] J.L. Thomas, W.L. Duax, A. Addlagatta, L. Scaccia, K.A. Frizzell, S.B. Carloni, Serine 124 completes the Tyr, Lys and Ser triad responsible for the catalysis of human type 1 3β-hydroxysteroid dehydrogenase, J. Mol. Endocrinol. 33 (1) (2004) 253–261.
[27] J.L. Thomas, R. Huether, V.L. Mack, L.A. Scaccia, R.C. Stoner, W.L. Duax, Structure/function of human type 1 3β-hydroxysteroid dehydrogenase: an intrasubunit disulfide bond in the Rossmann-fold domain and a Cys residue in the active site are critical for substrate and coenzyme utilization, J. Steroid Biochem. Mol. Biol. 107 (1–2) (2007) 80–87.
[28] J.L. Thomas, W.L. Duax, A. Addlagatta, S. Brandt, R.R. Fuller, W. Norris, Structure/function relationships responsible for coenzyme specificity and the isomerase activity of human type 1 3β-hydroxysteroid dehydrogenase/isomerase, J. Biol. Chem. 278 (37) (2003) 35483–35490.
[29] J.L. Thomas, W.E. Nash, R.C. Strickler, Physiologic 3β-hydroxy-5-ene-steroid substrates bind to 3β-hydroxysteroid dehydrogenase without the prior binding of cofactor, J. Steroid Biochem. Mol. Biol. 58 (2) (1996) 211–216.
[30] J.R. Pasqualini, The selective estrogen enzyme modulators in breast cancer: a review, Biochim. Biophys. Acta 1654 (2) (2004) 123–143.
[31] J. Simard, F. Durocher, F. Mebarke, C. Turgeon, R. Sanchez, Y. Labrie, J. Couet, C. Trudel, E. Rheaume, Y. Morel, V. Luu-The, F. Labrie, Molecular biology and genetics of the 3β-hydroxysteroid dehydrogenase/Δ5-Δ4 isomerase gene family, J. Endocrinol. 150 (Suppl.) (1996) S189–S207.
[32] R.G. Christiansen, H.C. Neumann, U.J. Salvador, M.R. Bell, H.P. Schane Jr., J.E. Creange, G.O. Potts, A.J. Anzalone, Steroidogenesis inhibitors. 1. Adrenal inhibitory and interceptive activity of trilostane and related compounds, J. Med. Chem. 27 (7) (1984) 928–931.
[33] G.O. Potts, J.E. Creange, H.R. Hardomg, H.P. Schane, Trilostane, an oral inhibitor of steroid biosynthesis, Steroids 32 (2) (1978) 257–267.
[34] D.T. Robinson, R.J. Earnshaw, R. Mitchell, P. Powles, R.S. Andrews, W.R. Robertson, The bioavailablity and metabolism of trilostane in normal subjects, a comparative study using high pressure liquid chromatography and quantitative cytochemical assays, J. Steroid Biochem. 21 (5) (1984) 601–605.
[35] D. Ghosh, M. Sawicki, V. Pletnev, M. Erman, S. Ohno, S. Nakajin, W.L. Duax, Porcine carbonyl reductase. Structural basis for a functional monomer in short chain dehydrogenases/reductases, J. Biol. Chem. 276 (21) (2001) 18457–18463.
[36] J. Singh, J.M. Thornton, Atlas of Protein Side-Chain Interactions, vol. 1, IRL Press, Oxford, 1992, pp. 244–245, 264–265.
[37] J.L. Thomas, V.L. Mack, J.A. Glow, D. Moshkelani, K.M. Bucholtz, Structure/function of the inhibition of human 3β-hydroxysteroid dehydrogenase type 1 and type 2 by trilostane, J. Steroid Biochem. Mol. Biol. 111 (1–2) (2008) 66–73.
[38] M. Samson, F. Labrie, V. Luu-The, Inhibition of human type 1 3β-hydroxysteroid dehydrogenase/Δ^5-Δ^4-isomerase expression using siRNA, J. Steroid Biochem. Mol. Biol. 94 (1–3) (2005) 253–257.